

WMAP Constraints, SUSY Dark Matter and Implications for the Direct Detection of SUSY

Utpal Chattopadhyay^{1(a)}, Achille Corsetti^{2(b)} and Pran Nath^{3(b)}

(a) *Department of Theoretical Physics, Indian Association for the Cultivation of Science, Jadavpur, Kolkata 700032, India*

(b) *Department of Physics, Northeastern University, Boston, MA 02115-5005, USA*

Abstract

Recently WMAP has measured the cosmological parameters to a much greater accuracy. We analyze the implications of this more precise measurement for supersymmetric dark matter and for the direct detection of supersymmetry at accelerators. We consider mSUGRA including also the hyperbolic branch (HB) in the radiative breaking of the electroweak symmetry. On the part of the hyperbolic branch where the lightest neutralino is dominantly a higgsino rather than being mostly a bino, the relic density constraints are satisfied by coannihilation with the next lightest neutralino and the light chargino. Including this branch the lightest neutralino mass satisfies $m_{\chi_1^0} \leq 1200$ GeV for $\tan \beta \leq 50$. Constraints of $b \rightarrow s + \gamma$, of $g_\mu - 2$, and of $B_s^0 \rightarrow \mu^+ \mu^-$ are also analyzed. It is shown that the neutralino-proton cross section in each case will fall within the reach of dark matter experiments. Possibility for the direct detection of supersymmetry is discussed in the allowed regions of the parameter space consistent with WMAP constraints. A brief discussion of the hyperbolic branch and focus point region (HB/FP) is also given. .

1 Introduction

Recently the Wilkinson Microwave Anisotropy Probe (WMAP) has measured some of the cosmological parameters with significantly greater precision[1, 2]. Specifically, WMAP gives the matter density of the universe so that $\Omega_m h^2 = 0.135_{-0.009}^{+0.008}$ and gives the baryon density so that $\Omega_b h^2 = 0.0224 \pm 0.0009$, where $\Omega_{m,b} = \rho_{m,b}/\rho_c$ where $\rho_{m,b}$ is the matter (baryon) density and ρ_c is the mass density needed to close the universe and h is the Hubble parameter in units of 100km/s/Mpc . Assuming the difference of the two is cold dark matter (CDM) one finds the CDM density in the universe according to WMAP is now given by $\Omega_{CDM} h^2 = 0.1126_{-0.009}^{+0.008}$. In

¹E-mail: tpuc@iacs.res.in

²E-mail: corsetti@neu.edu

³E-mail: nath@neu.edu

this paper we analyze the constraint of the WMAP results for supersymmetric dark matter. For the analysis we will focus on the mSUGRA model[3] and analyze the allowed range of the parameter space consistent with the WMAP relic density constraint. The above requires taking account of the full range of the hyperbolic branch of radiative breaking of the electroweak symmetry[4]. The mSUGRA model is characterized by the parameters $m_0, m_{1/2}, A_0, \tan\beta$ where m_0 is the universal scalar mass, $m_{1/2}$ is the universal gaugino mass, A_0 is the universal trilinear coupling and $\tan\beta$ is defined by $\tan\beta = \langle H_2 \rangle / \langle H_1 \rangle$ where H_2 gives mass to the up quark and the H_1 gives mass to the down quark and the lepton. In the analysis we will also consider the $b \rightarrow s\gamma$ constraint and the $g_\mu - 2$ constraint. $\tan\beta$ in the analysis will range up to values of 50 and it is known[4] that for values of $\tan\beta$ which are large or even moderately large that radiative breaking of the electroweak symmetry lies on the hyperbolic branch. To make the discussion clearer we review briefly radiative breaking of the electroweak symmetry and discuss how the hyperbolic branch arises in such a breaking. One can illustrate this phenomenon analytically for the case when the b quark couplings can be neglected. In this case one of the constraints of radiative symmetry breaking determines the Higgs mixing parameter μ so that[4]

$$C_1 m_0^2 + C_3 m_{1/2}^2 + C_2 A_0^2 + \Delta\mu_{loop}^2 = \mu^2 + \frac{1}{2} M_Z^2 \quad (1)$$

Here,

$$m'_{1/2} = m_{1/2} + \frac{1}{2} A_0 \frac{C_4}{C_3}, \quad C'_2 = C_2 - \frac{1}{4} \frac{C_4^2}{C_3} \quad (2)$$

and,

$$C_1 = \frac{1}{t^2 - 1} \left(1 - \frac{3D_0 - 1}{2} t^2\right), \quad C_2 = \frac{t^2}{t^2 - 1} k$$

$$C_3 = \frac{1}{t^2 - 1} (g - t^2 e), \quad C_4 = -\frac{t^2}{t^2 - 1} f, \quad \Delta\mu_{loop}^2 = \frac{\Sigma_1 - t^2 \Sigma_2}{t^2 - 1} \quad (3)$$

$\Delta\mu^2$ is the loop correction. $\Sigma_{1,2}$ is as defined in Ref.[4], $t = \tan\beta$ and the functions e, f, g, k are as defined in Ref.[5]. Further, $D_0 = 1 - (m_t/m_f)^2$ and $m_f \simeq 200 \sin\beta$ GeV.

For small to moderate values of $\tan\beta$ the loop corrections are typically small and further the renormalization group analysis shows that $C'_2 > 0$ and $C_3 > 0$. For such values of $\tan\beta$ where the loop corrections have reduced scale dependence one finds $C_1 > 0$ independent of any scale choice Q for having the radiative electroweak symmetry breaking (EWSB). In this circumstance one finds that the radiative

symmetry breaking constraint demands that the allowed set of soft parameters m_0 and $m'_{\frac{1}{2}}$ for a given value of μ lie on the surface of an ellipsoid. This condition then places an upper bound on sparticle masses for a given value of Φ which is the fine tuning parameter defined by $\Phi = \frac{\mu^2}{M_Z^2} + \frac{1}{4}$ [4]. This is the ellipsoidal branch of radiative breaking of the electroweak symmetry[4]. However, it was found in Ref.[4] that for typically larger $\tan \beta$ ($\gtrsim 7$) when the loop corrections to μ are significant along with a significant degree of its variation with the scale Q , the above scenario does not necessarily hold. One way to see this phenomenon is to choose a value of the running scale Q_0 at which the loop corrections to μ are minimized. One finds then that in some parts of the parameter space where m_0 and $m_{1/2}$ are relatively larger the minimization scale Q_0 occurs in such a region that it leads to a switch in the sign of C_1 , i.e. $\text{sign}(C_1(Q_0)) = -1$. In this circumstance one finds that the radiative symmetry breaking condition takes the form

$$\frac{m_{1/2}^2}{\alpha^2(Q_0)} - \frac{m_0^2}{\beta^2(Q_0)} \simeq \pm 1 \quad (4)$$

where the sign \pm is determined by the condition $\text{sign}((\Phi + \frac{1}{4})M_Z^2 - C'_2 A_0^2) = \pm$ and where

$$\alpha^2 = \frac{|(\Phi_0 + \frac{1}{4})M_Z^2 - C'_2 A_0^2|}{|C_3|}, \quad \beta^2 = \frac{|(\Phi_0 + \frac{1}{4})M_Z^2 - C'_2 A_0^2|}{|C_1|} \quad (5)$$

From the above we see that the presence of the relative minus sign leads to a drastically different constraint on the soft parameters due to constraint of the radiative breaking of the electroweak symmetry. Here for fixed values of A_0 one finds that m_0 and $m'_{\frac{1}{2}}$ lie on a hyperbola and thus these parameters can get large for fixed values of μ or for fixed values of the fine tuning parameter Φ . This is the high zone of the hyperbolic branch of radiative breaking of the electroweak symmetry[4]. Remarkably, the soft parameters can be quite large even while the value of Φ or μ can be chosen to be significantly small. This is a feature which gives a significantly different type of mixing of gauginos and higgsinos than the usually explored regions of the minimal supergravity model. In the high zone of the hyperbolic branch when $m_{\frac{1}{2}} \gg \mu$, an inversion phenomenon takes place, and the neutralino mass becomes essentially μ . The above has a drastic effect on sparticle spectrum and on supersymmetry phenomenology which we discuss below.

2 Sparticle Spectrum in the Inversion Region of the Hyperbolic Branch

As discussed in Sec.1 the constraints on m_0 and $m_{\frac{1}{2}}$ for fixed μ for the hyperbolic branch are very different than for the usual (ellipsoidal) scenario. Here since m_0 and $m_{\frac{1}{2}}$ can get large for fixed μ one finds that the squark and slepton masses get very heavy and may lie in the several TeV range (The feature of large m_0 is shared by the focus point region of mSUGRA models[6]). We consider here a specific part of the hyperbolic branch where $m_{\frac{1}{2}} \gg \mu \gg M_Z$. In this scenario then one finds the two lightest neutralino states χ_1^0, χ_2^0 and the light chargino state χ_1^\pm are essentially degenerate, each with mass $\sim |\mu|$. We will call this phenomenon "inversion" in that the lightest neutralino switches from being mostly a Bino to being purely a higgsino. In fact, this is also the case for the second lowest neutralino and the lighter chargino since all of them have a common mass μ to the leading order. The degeneracy is lifted when corrections $O(M_Z^2/M_{1,2})$ and $O(M_Z^2/\mu)$ are included. The remaining sparticle spectrum consisting of quarks, sleptons, gluino and the remaining charginos and neutralinos are significantly higher and in principle could lie in the several TeV range and perhaps beyond the reach of even the LHC. Thus the prospects of observing supersymmetry depends on our ability to observe the particles χ_1^0, χ_2^0 and χ_1^\pm in addition to the observation of the light Higgs boson. Including the lowest order perturbation corrections $O(M_Z^2/M_{1,2})$ and $O(M_Z^2/\mu)$ the masses of these three lowest mass states in the inversion region at the tree level are given by

$$\begin{aligned}
 M_{\chi_1^0} &= \mu - \frac{M_Z^2}{2}(1 - \sin 2\beta) \left[\frac{\sin^2 \theta_W}{M_1 - \mu} + \frac{\cos^2 \theta_W}{M_2 - \mu} \right] \\
 M_{\chi_2^0} &= \mu + \frac{M_Z^2}{2}(1 + \sin 2\beta) \left[\frac{\sin^2 \theta_W}{M_1 + \mu} + \frac{\cos^2 \theta_W}{M_2 + \mu} \right] \\
 M_{\chi_1^\pm} &= \mu + \frac{M_W^2 \cos^2 \beta}{\mu} - \frac{M_W^2}{\mu} \frac{(M_2 \cos \beta + \mu \sin \beta)^2}{(M_2^2 - \mu^2)}
 \end{aligned} \tag{6}$$

Thus for $\mu > 0$ the mass pattern that emerges is

$$m_{\chi_1^0} < m_{\chi_1^\pm} < m_{\chi_2^0} \tag{7}$$

The quantities that are relevant for the observability of these sparticles are the mass differences

$$\Delta M^\pm = m_{\chi_1^\pm} - m_{\chi_1^0}, \quad \Delta M^0 = m_{\chi_2^0} - m_{\chi_1^0} \tag{8}$$

While $m_{\chi_1^\pm}$, $m_{\chi_1^0}$, and $m_{\chi_2^0}$ masses lie in the several hundred GeV to TeV (above TeV) range the mass differences ΔM^\pm are much smaller and lie in the range 1-10 GeV. The mass differences can receive loop corrections[7, 8] which can be as much as 25% or more. However, these corrections do not modify the general picture of this scenario. The above leads to some important constraints on what may be observed experimentally.

3 Coannihilation, relic density, and detection rates with WMAP Constraints

We discuss now the WMAP constraints on SUSY dark matter and also investigate if such dark matter will be accessible to direct detection. This issue is of great importance as there are on going dark matter experiments[9, 10, 11, 12] and also experiments planned for the future[13, 14] to detect dark matter. In the analysis we will use a 2σ constraint on the WMAP[1, 2] result for CDM, i.e., we take

$$\Omega_\chi h^2 = 0.1126_{-0.018}^{+0.016} \quad (9)$$

Many interesting theoretical investigations in the analysis of supersymmetric dark matter have been carried out over the years[15, 8, 16, 17]. These include investigations of the effects of the variations of uncertainties in the relic density and wimp velocity on the detection rates[18], effects of nonuniversalities in the Higgs sector[19, 20] and in the gaugino sector[21, 22], effects of CP phases[23], and the effects of Yukawa unification[24, 25]. More recently the effects of coannihilation on supersymmetric dark matter have been analyzed[26, 27, 28, 24, 29, 30, 31, 32]. This effect becomes important when the mass of the next to the lightest supersymmetric particle (nlsp) is close to the mass of the lightest supersymmetric particle (lsp) at the time when the lsp's decouple from the background. In such a situation the coannihilation processes involving lsp-nlsp and the nlsp-nlsp annihilation must be taken into account. The quantity of interest is the number density $n_a = \sum n_a$ where a runs over the particle types that enter in coannihilation, and n obeys the Boltzmann equation

$$\frac{dn}{dt} = -3Hn - \langle \sigma_{eff} v \rangle (n^2 - n_0^2) \quad (10)$$

where H is the Hubble parameter, n_0 is the equilibrium number density and σ_{eff} is the effective total cross section defined by

$$\sigma_{eff} = \sum \sigma_{ab} r_a r_b \quad (11)$$

where σ_{ab} is the annihilation cross section of particle a with particle b, and $r_a = n_{0a}/n_0$ where n_{0a} is the density of particles of species a at equilibrium. After the freeze out the nlsp's decay to the lsp and thus n becomes the number density of the lsp. It was shown that in mSUGRA one naturally has coannihilation with the sleptons when the neutralino mass extends to masses beyond 150-200 GeV with processes of the type $\chi\tilde{\ell}_R^a \rightarrow \ell^a\gamma, \ell^a Z, \ell^a h$, $\tilde{\ell}_R^a\tilde{\ell}_R^b \rightarrow \ell^a\ell^b$, and $\tilde{\ell}_R^a\tilde{\ell}_R^{b*} \rightarrow \ell^a\bar{\ell}^b, \gamma\gamma, \gamma Z, ZZ, W^+W^-, hh$ where \tilde{l} is essentially a $\tilde{\tau}$. The above coannihilation processes extend the allowed neutralino range up to 700 GeV[28]. We will show that remarkably the relic density constraints can be satisfied on the hyperbolic branch also by coannihilation. However, on the hyperbolic branch the coannihilation is of an entirely different nature. Specifically in the inversion region the dominant coannihilation is the $\chi_1^0 - \chi_1^\pm$ coannihilation followed by $\chi_1^0 - \chi_2^0$ coannihilation, and by $\chi_1^+ - \chi_1^-$ and by $\chi_1^\pm - \chi_2^0$ coannihilations. Some of the dominant processes that contribute to the above coannihilation processes are[33]

$$\begin{aligned}\chi_1^0\chi_1^+, \chi_2^0\chi_1^+ &\rightarrow u_i\bar{d}_i, \bar{e}_i\nu_i, AW^+, ZW^+, W^+h \\ \chi_1^+\chi_1^-, \chi_1^0\chi_2^0 &\rightarrow u_i\bar{u}_i, d_i\bar{d}_i, W^+W^-\end{aligned}\quad (12)$$

Since the mass difference between the states χ_1^+ and χ_1^0 is the smallest the $\chi_1^0\chi_1^+$ coannihilation dominates.

In the analysis we include the $b \rightarrow s\gamma$ constraint[34] and the $g_\mu - 2$ constraint[35]. The constraint arising from $B_s^0 \rightarrow \mu^+\mu^-$ for large $\tan\beta$ is also discussed. The analysis of Ref.[36] gives two estimates for the difference $a_\mu^{exp} - a_\mu^{SM}$: These are [I] $a_\mu^{exp} - a_\mu^{SM} = 1.7(14.2) \times 10^{-10}$ [37, 36] and [II] $a_\mu^{exp} - a_\mu^{SM} = 24.1(14.0) \times 10^{-10}$ [38, 36]. These estimates also include corrections from scalar mesons to the muon anomaly computed in Ref.[36]. Estimate [I] corresponds to essentially a perfect agreement and does not put any effective upper limit constraints on the parameter space. In our analysis we consider a 1.5σ range around the central value of estimate [II], i.e., we choose $3.1 \times 10^{-10} \leq (a_\mu^{exp} - a_\mu^{SM}) \leq 45.1 \times 10^{-10}$. We attribute the difference to supersymmetry[39]. In Fig. 1(a) we exhibit the allowed parameter space in the $m_0 - m_{\frac{1}{2}}$ plane which satisfies the relic density constraint consistent with Eq.(9) for the case $\tan\beta = 10$ and $\mu > 0$. The filled dark circles indicate the regions which are consistent with the relic density constraints. We note that this region includes a lower branch which is the conventional branch where the relic density constraints are satisfied due to coannihilation with staus. For the case of Fig. 1(a) this extends to $m_{\frac{1}{2}}$ of about 800 GeV and $m_{\chi_1^0}$ of about 300 GeV as can be seen

more clearly from Fig. 1(b). However, there is also an upper branch where the allowed values of $m_{\frac{1}{2}}$ consistent with relic density run up to the upper limit chosen i.e. 10 TeV. The corresponding neutralino mass, however, runs up only to 1200 GeV because of the phenomenon of inversion discussed in Sec.2. As can be seen from Fig. 1(b) relic density constraints consistent with the WMAP constraints can be satisfied in the inversion region for significantly large values of the neutralino mass and values of m_0 up to 16 TeV. The phenomenon of inversion can be seen more clearly in Fig. 1(c) where points consistent with the WMAP constraints are exhibited in the $m_{\frac{1}{2}} - m_{\chi_1^0}$ plane. The imposition of the $g_\mu - 2$ constraint [II] eliminates all of the inversion region and much of the remaining region of the high zone of the hyperbolic branch. However, essentially all of the region allowed by the relic density constraints is valid if we consider the $g_\mu - 2$ constraint [I]. In Figs. 2(a), 2(b), 2(c) we give an analysis similar to that of Figs.1(a), 1(b), and 1(c) except that $\tan\beta = 30$. Similarly in Figs.3(a), 3(b), and 3(c) we give an analysis similar to that of Figs.1(a), 1(b), and 1(c) except $\tan\beta = 50$. For the cases of $\tan\beta = 30$ and $\tan\beta = 50$ the $b \rightarrow s\gamma$ constraint is also displayed. In these cases the region below the curves labelled $b \rightarrow s\gamma$ is the disallowed region.

For large $\tan\beta$ the constraint from $B_s^0 \rightarrow \mu^+\mu^-$ is also of interest[40, 41]. In the standard model the branching ratio for this process is $B(\bar{B}_s^0 \rightarrow \mu^+\mu^-) = (3.1 \pm 1.4) \times 10^{-9}$ ($V_{ts} = 0.04 \pm 0.002$) while the current limit from experiment is $B(\bar{B}_s^0 \rightarrow \mu^+\mu^-) < 2.6 \times 10^{-6}$. The current estimates are that RUNII of the Tevatron will eventually increase the sensitivity for this process to the limit 10^{-8} [41] which still falls short of reaching the branching ratio for this process in the standard model. However, it turns out that in supersymmetry this branching ratio is dominated by the so called counterterm diagram and the contribution from this diagram gives the branching ratio a dependence on $\tan\beta$ of $\tan^6\beta$ for large $\tan\beta$. As a consequence the $B(\bar{B}_s^0 \rightarrow \mu^+\mu^-)$ branching ratio in supersymmetry can get larger than the standard model value by as much as a factor of 10^3 which brings it within reach of RUNII of the Tevatron. However, the $B(\bar{B}_s^0 \rightarrow \mu^+\mu^-)$ branching ratio in supersymmetry is very sensitive to the sparticle spectrum and falls sharply as the sparticle spectrum becomes heavy. In Fig. 4 we give a plot of the $B(\bar{B}_s^0 \rightarrow \mu^+\mu^-)$ constraint in the $m_0 - m_{\frac{1}{2}}$ plane. We find that the current experimental constraint on $B(\bar{B}_s^0 \rightarrow \mu^+\mu^-)$ does not eliminate any relevant part of the parameter space while $B(\bar{B}_s^0 \rightarrow \mu^+\mu^-) = 10^{-8}$ can explore the parameter space in m_0 up to 700 GeV and in $m_{\frac{1}{2}}$ up to about 500 GeV. This mass range is far too small to have

any influence on the region of the hyperbolic branch we are focussing on in this analysis. For this reason this constraint is not very effective in the present analysis.

A quantity of great interest is the spin independent neutralino-proton cross section $\sigma_{\chi_1^0 p}(SI)$ on which experimental limits exist from the current dark matter experiments so that $\sigma_{\chi_1^0 p}(SI) \leq 10^{-42} \text{cm}^2$. In Fig. 5(a) we give a plot of $\sigma_{\chi_1^0 p}(SI)$ for $\tan\beta = 10$ and $\mu > 0$. In Fig. 5(a) the lower rapidly falling curve that terminates at $m_{\chi_1^0} = 300$ GeV is the branch on which staus coannihilation occurs. The upper curve arises from the low zone of the hyperbolic branch while the patch to the right is the one that arises from the inversion region of the hyperbolic branch. For values of neutralino masses below 300 GeV the $\sigma_{\chi_1^0 p}(SI)$ cross section arising from the upper curve in Fig.1(a) is much larger than the one arising from the lower branch where the relic density constraints are satisfied due to neutralino-stau coannihilation. We also note that in Fig. 5(a) the patch to the right indicates that the scalar cross sections are quite significant even though one is in the inversion region. Thus although the direct detection of supersymmetry in the inversion region is more difficult, the neutralino-proton scalar cross sections are still substantial. In the future dark matter detectors[13] will be able to achieve a sensitivity of up to 10^{-45}cm^2 . We note that a significant part of the parameter space of Fig. 5(a) will be probed by these detectors. In Fig. 5(b) we give a plot of the spin dependent neutralino-proton cross section $\sigma_{\chi_1^0 p}(SD)$ for $\tan\beta = 10$ $\mu > 0$. A comparison of Fig. 5(a) and Fig. 5(b) shows that the spin dependent cross section is typically much larger than the spin independent cross section by 3-4 orders of magnitude. A similar analysis for the case $\tan\beta = 30$ is given in Fig. 6(a) and Fig. 6(b) while for the case $\tan\beta = 50$ is given in Fig. 7(a) and Fig. 7(b). The conclusions for these cases are very similar to the conclusions drawn from Fig. 5(a) and Fig. 5(b). Based on these analyses one finds that for $\tan\beta \leq 50$, the neutralino mass range consistent with the WMAP constraints on the branch corresponding to neutralino-stau coannihilation is $m_{\chi_1^0} \leq 500$ GeV and $m_{\chi_1^0} \leq 1200$ GeV for the high zone of the hyperbolic branch where the relic density constraints are satisfied due to coannihilation with the next to lightest neutralino and the light chargino. These constraints remain intact under the imposition of the $g_\mu - 2$ constraint [I] but the constraint arising from the inversion region of the hyperbolic branch is removed by imposition of the $g_\mu - 2$ constraint [II].

4 WMAP Constraints and Discovering SUSY at accelerators

The analysis of Sec.3 shows that Eq.(9) constraints the parameter space very strigently. For the usually explored parameter space of minimal supergravity where relic density is satisfied in the region of neutralino-stau coannihilation as well as in the low zone of the hyperbolic branch with a moderate amount of higgsino in the lsp (i.e. without inversion), one finds that the neutralino mass now has an upper limit of about 500 GeV for $\tan\beta \leq 50$ and m_0 lies in the few hundred GeV range. For this case the corresponding sparticle spectrum should all be accessbile at the LHC and perhaps some of it may be accessible at RUNII at the Tevatron. Also there are some interesting signals for this branch at the NLC[42]. However, on the inversion region of the hyperbolic branch of radiative breaking of the electroweak symmetry, m_0 and $m_{\frac{1}{2}}$ can get as large as 10 TeV or even higher. In this case the squarks and the sleptons would lie in the several TeV region and hence they would be beyond the reach of even the LHC. The light particles in this scenario will be the two lightest neutralinos and the light chargino. However, the signals for their detection would be significantly different than for the normal scenarios. Specifically, in the inversion region of the hyperbolic branch the mass differences among χ_1^0 , χ_1^\pm and χ_2^0 are so small that the usual signals discussed for the detection of supersymmetry would not apply[43].

Situations of the type above have been discussed before in Ref.[44] in the context of string models and in Ref.[45] in the context of Wino lsp scenarios while the experimental search for charginos mass-degenerate with the lightest neutralinos has been analyzed in Ref.[46]. Here the mass scales are significantly different. Thus, for example, in the analyzes of Ref[45] the mass difference of the chargino and the nearly degenerate neutralino is in the range of $O(100)$ MeV which allows for charged particle tracks in the detector of the order of few centimeters arising from the decay of the chargino to neutralino such as $\chi_1^+ \rightarrow \chi_1^0 l^+ \nu_l$, and $\chi_1^+ \rightarrow \chi_1^0 l^+ \pi^+$. In the present scenario the chargino and neutralino masses are in the several hundred GeV to 1-2 TeV range and their mass difference lie in the range of 1-10 GeV. The mass differences are such that the chargino will always decay in the detector and the track length will be too small to be visible. Further, the conventional tripleptonic signal[47] would yield leptons with energies only in the few GeV region to provide a useful signal at the LHC[48]. In Ref.[44] it is argued that charginos nearly degenerate with neutralinos may be observable in

e^+e^- colliders via observation of hard photons in the process $e^+e^- \rightarrow \gamma\chi_1^+\chi_1^-$. However, a more detailed analysis for the detection of supersymmetry in collider experiments is needed for the scenario discussed here. On the whole, the prospects for the detection of SUSY signals at accelerators in this scenario look difficult. On the other hand quite interestingly this scenario does provide a sufficient amount of dark matter to populate the universe and a part of the parameter space of this branch does yield spin independent neutralino-proton cross sections which lie in the range of observability of dark matter detectors. We emphasize that much of the high zone of the hyperbolic branch and specifically all of the inversion region on the hyperbolic branch can be eliminated if the $g_\mu - 2$ constraint [II] holds. However, the high zone of the hyperbolic branch would not be significantly constrained if the $g_\mu - 2$ constraint [I] holds. This points to the importance of getting an unambiguous determination of the leading order (LO) hadronic correction to $g_\mu - 2$.

We comment now briefly on the relation of the hyperbolic branch to the focus point region[6]. As discussed in Sec.1 we showed that one can find solutions to radiative breaking of the electroweak symmetry where m_0 and $m_{1/2}$ can get large while μ remains fixed and relatively small. These solutions constitute the hyperbolic branch. A part of this region also includes the so called focus point region. Thus the focus point region is limited to relatively small values of $m_{1/2}$ and consequently m_0 is also limited from getting very large because of the radiative symmetry breaking constraint relative to the case of the hyperbolic branch. Thus the focus point region (FP) is truly a subset of the hyperbolic branch (HB). A further discussion of this point can be found in Ref.[49] where the acronym HB/FP is used to describe this region.

5 Conclusion

The recent WMAP determination of the cosmological parameters, specifically $\Omega_m h^2$ and $\Omega_b h^2$, to a much better accuracy than earlier determinations has important consequences for the observation of supersymmetric dark matter and also for the direct detection of supersymmetry. In our analysis we have identified the difference $\Omega_m h^2 - \Omega_b h^2$ as arising from relic neutralinos and analyzed this possibility within mSUGRA. One finds that for the region of the parameter space where the relic density constraints are satisfied due to the neutralino-stau coannihilation, the neutralino mass limit is now reduced to $m_{\chi_1^0} \leq 500$ GeV for $\tan\beta \leq 50$. The

spectrum in this case will all be accessible at the LHC with the possibility of some sparticles also being accessible at RUNII of the Tevatron. Also some interesting signals may arise in this case at the NLC. On the high zone of the hyperbolic branch including the inversion region, the WMAP constraints are satisfied remarkably to a very high value of the neutralino mass, i.e., up to $m_{\chi_1^0} \leq 1200$ GeV for $\tan\beta \leq 50$. The satisfaction of the relic density even for such large neutralino masses comes about because of coannihilation processes exhibited in Eq.(12). As discussed in Sec.2, in the high zone of the hyperbolic branch m_0 and $m_{\chi_1^0}$ can get very large and some of the sparticle spectrum may lie outside the reach of even the LHC. Thus the squarks, sleptons and gluinos may be too massive to be accessible even at the LHC. Thus the direct observation of SUSY would be very challenging if the inversion region of the hyperbolic branch is realized. In this region the only light particles, aside from the light Higgs boson h^0 , are the sparticles $\chi_1^\pm, \chi_1^0, \chi_2^0$. The mass splittings among them are typically O(10) GeV and thus their detection poses a challenge. Luckily much of the hyperbolic branch and all of the inversion region of the hyperbolic branch can be eliminated by a $g_\mu - 2$ signal. This is what happens when we impose the $g_\mu - 2$ constraint [II]. However, imposition of the $g_\mu - 2$ constraint [I] essentially leaves all of the region of the hyperbolic branch including the inversion region intact. This points to the need to achieve an unambiguous $g_\mu - 2$ constraint by reducing the errors in the leading order (LO) hadronic contributions. We also computed the spin independent neutralino proton cross section $\sigma_{\chi_1^0 p}(SI)$ and found that it lies in the range $10^{-46} - 10^{-43} cm^2$. A significant part of this range will be accessible to the future dark matter experiments[13, 14]. Implications of WMAP constraints for supersymmetry have also been reported in Ref.[50].

Acknowledgments

Conversations with H. Baer, J. Feng and D. Wood related to topics discussed here are acknowledged. This research was supported in part by NSF grant PHY-0139967

References

- [1] C. L. Bennett *et al.*, arXiv:astro-ph/0302207.
- [2] D. N. Spergel *et al.*, arXiv:astro-ph/0302209.
- [3] A.H. Chamseddine, R. Arnowitt and P. Nath, *Phys. Rev. Lett.* **49**, 970

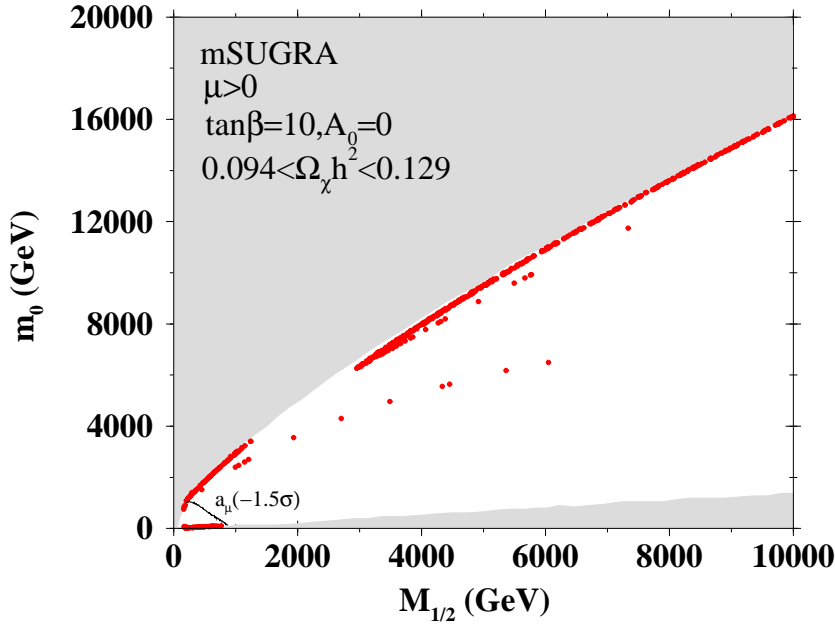
- (1982); R. Barbieri, S. Ferrara and C.A. Savoy, *Phys. Lett. B* **119**, 343 (1982); L. Hall, J. Lykken, and S. Weinberg, *Phys. Rev. D* **27**, 2359 (1983); P. Nath, R. Arnowitt and A.H. Chamseddine, *Nucl. Phys. B* **227**, 121 (1983).
- [4] K.L. Chan, U. Chattopadhyay and P. Nath, *Phys. Rev. D* **58**, 096004 (1998).
- [5] L.E. Ibanez, C. Lopez and C. Munoz, *Nucl. Phys.* **B256** (1985) 218-252.
- [6] J. L. Feng, K. T. Matchev and T. Moroi, *Phys. Rev. D* **61**, 075005 (2000); *Phys. Rev. Lett.* **84**, 2322 (2000) [arXiv:hep-ph/9908309].
- [7] D. Pierce and A. Papadopoulos, *Phys. Rev. D* **50**, 565 (1994); *Nucl. Phys. B* **430**, 278 (1994); A. B. Lahanas, K. Tamvakis and N. D. Tracas, *Phys. Lett. B* **324**, 387 (1994)
- [8] M. Drees, M. M. Nojiri, D. P. Roy and Y. Yamada, *Phys. Rev. D* **56**, 276 (1997);
- [9] R. Belli et.al., *Phys. Lett.***B480**,23(2000), "Search for WIMP annual modulation signature: results from DAMA/NAI-3 and DAMA/NAI-4 and the global combined analysis", DAMA collaboration preprint INFN/AE-00/01, 1 February, 2000.
- [10] R. Abusaidi et.al., *Phys. Rev. Lett.***84**, 5699(2000), "Exclusion Limits on WIMP-Nucleon Cross-Section from the Cryogenic Dark Matter Search", CDMS Collaboration preprint CWRU-P5-00/UCSB-HEP-00-01 and astro-ph/0002471.
- [11] L. Baudis, A. Dietz, B. Majorovits, F. Schwamm, H. Strecker and H.V. Klapdor-Kleingrothaus, *Phys. Rev.* **D63**,022001 (2001).
- [12] A. Benoit *et al.*, arXiv:astro-ph/0206271.
- [13] H.V. Klapdor-Kleingrothaus, et.al., "GENIUS, A Supersensitive Germanium Detector System for Rare Events: Proposal", MPI-H-V26-1999, hep-ph/9910205.
- [14] D. Cline *et al.*, "A Wimp Detector With Two-Phase Xenon," *Astropart. Phys.* **12**, 373 (2000).

- [15] K. Greist, Phys. Rev. **D38**, 2357(1988); J. Ellis and R. Flores, Nucl. Phys. **B307**, 833(1988); R. Barbieri, M. Frigeni and G. Giudice, Nucl. Phys. **B313**, 725(1989); A. Bottino et.al., **B295**, 330(1992); M. Drees and M.M. Nojiri, Phys. Rev.**D48**,3483(1993); V.A. Bednyakov, H.V. Klapdor-Kleingrothaus and S. Kovalenko, Phys. Rev.**D50**, 7128(1994); P. Nath and R. Arnowitt, Phys. Rev. Lett. **74**, 4592(1995); R. Arnowitt and P. Nath, Phys. Rev. **D54**, 2374(1996); E. Diehl, G.L. Kane, C. Kolda, J.D. Wells, Phys.Rev.**D52**, 4223(1995); L. Bergstrom and P. Gondolo, Astrop. Phys. **6**, 263(1996); H. Baer and M. Brhlik, Phys.Rev.**D57**,567(1998); J.D. Vergados, Phys. Rev. **D83**, 3597(1998); J.L. Feng, K. T. Matchev, F. Wilczek, Phys.Lett. **B482**, 388(2000); M. Brhlik, D. J. Chung and G. L. Kane, Int. J. Mod. Phys. D **10**, 367 (2001); V.A. Bednyakov and H.V. Klapdor-Kleingrothaus, Phys. Rev. D **63**, 095005 (2001); M. E. Gomez and J. D. Vergados, Phys. Lett. B **512**, 252 (2001); A. B. Lahanas, D. V. Nanopoulos and V. C. Spanos, Phys. Lett. B **518**, 94 (2001); J.L. Feng, K. T. Matchev, F. Wilczek, Phys. Rev. D **63**, 045024 (2001); V. D. Barger and C. Kao, Phys. Lett. B **518**, 117 (2001).
- [16] H. Baer, C. Balazs, A. Belyaev, J. K. Mizukoshi, X. Tata and Y. Wang, JHEP **0207**, 050 (2002) D. Auto, H. Baer, C. Balazs, A. Belyaev, J. Ferrandis and X. Tata, arXiv:hep-ph/0302155.
- [17] U. Chattopadhyay and P. Nath, Phys. Rev. D **66**, 093001 (2002)
- [18] P. Belli, R. Bernbei, A. Bottino, F. Donato, N. Fornengo, D. Prospero, and S. Scopel, Phys. Rev. **D61**, 023512(2000); M. Brhlik and L. Roszkowski, Phys. Lett. **B464**, 303(1999); A. Corsetti and P. Nath, Int. J. Mod. Phys. **A15**, 905(2000).
- [19] P. Nath and R. Arnowitt, Phys. Rev.**D56**, 2820(1997).
- [20] J. Ellis, A. Ferstl, K. A. Olive and Y. Santoso, arXiv:hep-ph/0302032.
- [21] A. Corsetti and P. Nath, Phys. Rev. D **64**, 125010 (2001); hep-ph/0005234; hep-ph/0011313.
- [22] A. Birkedal-Hansen and B. D. Nelson, arXiv:hep-ph/0211071.
- [23] U. Chattopadhyay, T. Ibrahim and P. Nath, Phys. Rev. **D60**,063505(1999); T. Falk, A. Ferstl and K. Olive, Astropart. Phys. **13**, 301(2000); S. Khalil,

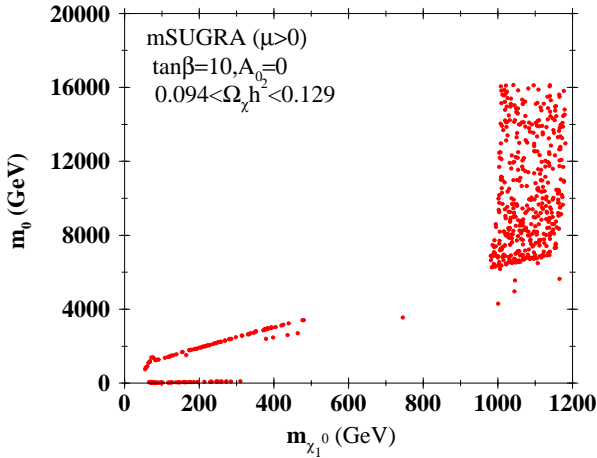
- Phys. Lett. **B484**, 98(2000); S. Khalil and Q. Shafi, Nucl.Phys. **B564**, 19(1999); K. Freese and P. Gondolo, hep-ph/9908390; S.Y. Choi, hep-ph/9908397.
- [24] M.E. Gomez, G. Lazarides and C. Pallis, Phys. Rev. **D61**, 123512(2000).
- [25] U. Chattopadhyay, A. Corsetti and P. Nath, Phys. Rev. D **66**, 035003 (2002) [arXiv:hep-ph/0201001]; U. Chattopadhyay and P. Nath, Phys. Rev. D **65**, 075009 (2002) [arXiv:hep-ph/0110341].
- [26] S. Mizuta and M. Yamaguchi, Phys. Lett. B **298**, 120 (1993) [arXiv:hep-ph/9208251].
- [27] J. R. Ellis, T. Falk and K. A. Olive, Phys. Lett. B **444**, 367 (1998) [arXiv:hep-ph/9810360].
- [28] J. R. Ellis, T. Falk, K. A. Olive and M. Srednicki, Astropart. Phys. **13**, 181 (2000) [Erratum-ibid. **15**, 413 (2001)] [arXiv:hep-ph/9905481].
- [29] R. Arnowitt, B. Dutta and Y. Santoso, Nucl. Phys. B **606**, 59 (2001) [arXiv:hep-ph/0102181].
- [30] J. R. Ellis, K. A. Olive and Y. Santoso, arXiv:hep-ph/0112113.
- [31] T. Nihei, L. Roszkowski and R. Ruiz de Austri, JHEP **0207**, 024 (2002) [arXiv:hep-ph/0206266].
- [32] V. A. Bednyakov, H. V. Klapdor-Kleingrothaus and V. Gronewold, arXiv:hep-ph/0208178.
- [33] J. Edsjo and P. Gondolo, Phys. Rev. D **56**, 1879 (1997) [arXiv:hep-ph/9704361].
- [34] S. Chen et.al. (CLEO Collaboration), Phys. Rev. Lett. **87**, 251807 (2001); H. Tajima, talk at the 20th International Symposium on Lepton-Photon Interactions", Rome, July 2001; R. Barate et.al., Phys. Lett. **B429**, 169(1998).
- [35] G. W. Bennett *et al.* [Muon g-2 Collaboration], Phys. Rev. Lett. **89**, 101804 (2002) [Erratum-ibid. **89**, 129903 (2002)] [arXiv:hep-ex/0208001].
- [36] S. Narison, arXiv:hep-ph/0303004.

- [37] M. Davier, S. Eidelman, A. Hocker and Z. Zhang, arXiv:hep-ph/0208177.
- [38] K. Hagiwara, A. D. Martin, D. Nomura and T. Teubner, Phys. Lett. B **557**, 69 (2003) [arXiv:hep-ph/0209187].
- [39] T. C. Yuan, R. Arnowitt, A. H. Chamseddine and P. Nath, Z. Phys. C **26**, 407 (1984); D. A. Kosower, L. M. Krauss and N. Sakai, Phys. Lett. B **133**, 305 (1983); J.L. Lopez, D.V. Nanopoulos, X. Wang, Phys. Rev. **D49**, 366(1994); U. Chattopadhyay and P. Nath, Phys. Rev. D **53**, 1648 (1996); T. Ibrahim and P. Nath, Phys. Rev. D **61**, 095008 (2000)
- [40] S. R. Choudhury and N. Gaur, Phys. Lett. B **451**, 86 (1999); K. S. Babu and C. Kolda, Phys. Rev. Lett. **84**, 228 (2000).
- [41] For more recent analyses see, A. Dedes, H. K. Dreiner, U. Nierste, and P. Richardson, Phys. Rev. Lett. **87**, 251804 (2001); R. Arnowitt, B. Dutta, T. Kamon and M. Tanaka, Phys. Lett. B **538** (2002) 121; S. Baek, P. Ko, and W. Y. Song, JHEP **0303**, 054 (2003); J. K. Mizukoshi, X. Tata and Y. Wang, Phys. Rev. D **66**, 115003 (2002); T. Ibrahim and P. Nath, Phys. Rev. D **67**, 016005 (2003) [arXiv:hep-ph/0208142].
- [42] T. Kamon, R. Arnowitt, B. Dutta and V. Khotilovich, arXiv:hep-ph/0302249.
- [43] A conversation with Jonathan Feng drawing our attention to this issue regarding the hyperbolic branch is acknowledged.
- [44] C. H. Chen, M. Drees and J. F. Gunion, Phys. Rev. Lett. **76**, 2002 (1996); Phys. Rev. D **55**, 330 (1997) [Erratum-ibid. D **60**, 039901 (1999)]
- [45] J. L. Feng, T. Moroi, L. Randall, M. Strassler and S. f. Su, Phys. Rev. Lett. **83**, 1731 (1999)
- [46] P. Abreu *et al.* [DELPHI Collaboration], Eur. Phys. J. C **11**, 1 (1999)
- [47] P. Nath and R. Arnowitt, Mod. Phys.Lett.**A2**, 331(1987); H. Baer and X. Tata, Phys. Rev.**D47**, 2739(1993); V. Barger and C. Kao, Phys. Rev. **D60**, 115015(1999).
- [48] CMS Collaboration: Technical Proposal. CERN/LHCC 94-38. LHCC/PI (1994).

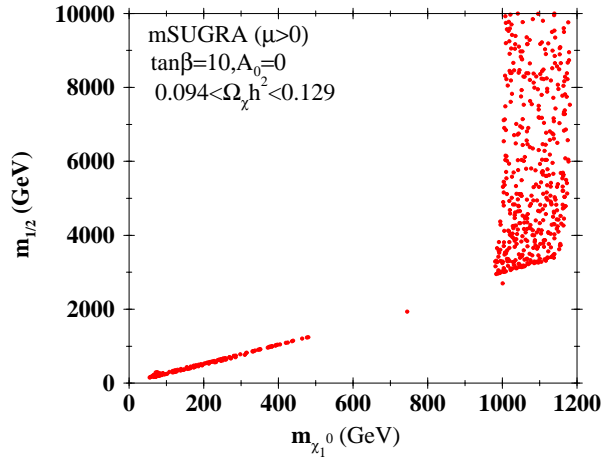
- [49] H. Baer, C. Balazs, A. Belyaev and J. O’Farrill, arXiv:hep-ph/0305191;
H. Baer, C. Balazs, A. Belyaev, T. Krupovnickas and X. Tata, arXiv:hep-ph/0304303; J. Ellis, K. A. Olive, Y. Santoso and V. C. Spanos, arXiv:hep-ph/0305212.
- [50] J. Ellis, K. A. Olive, Y. Santoso and V. C. Spanos, arXiv:hep-ph/0303043;
H. Baer and C. Balazs, arXiv:hep-ph/0303114; A. B. Lahanas and D. V. Nanopoulos, arXiv:hep-ph/0303130.



(a) A plot in the $m_0 - m_{\frac{1}{2}}$ plane of the allowed region consistent with electroweak symmetry breaking and the WMAP relic density constraints for the mSUGRA case. The input parameters are $A_0 = 0, \tan\beta = 10, \mu > 0$ and the relic density constraint imposed is of Eq.(9). The white region is the parameter space allowed by the electroweak symmetry breaking constraints while the shaded region is disallowed. The filled circles denote the region allowed by the relic density constraint. The filled circles just below the upper shaded region arise from the hyperbolic branch. $a_\mu^{SU5Y}(-1.5\sigma)$ contour is the black line.

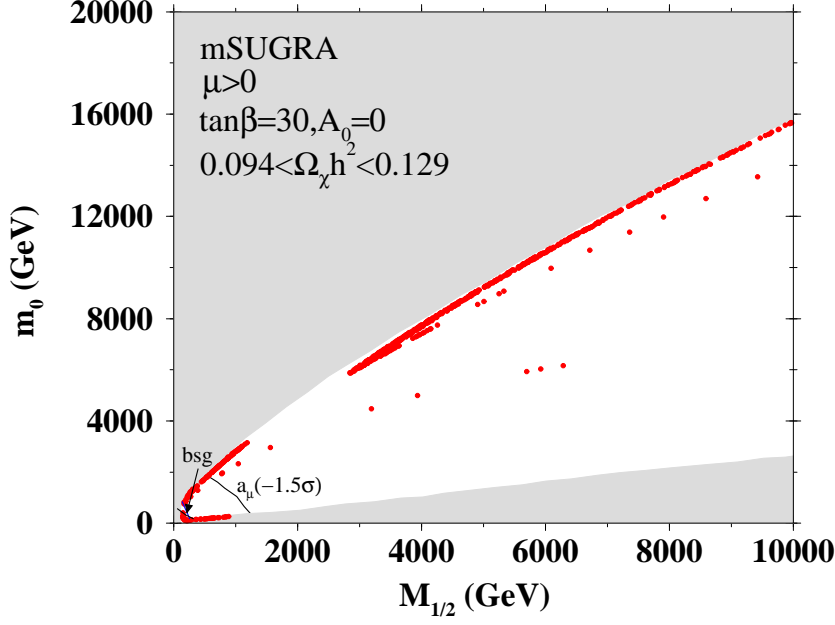


(b) A plot in the $m_0 - m_{\chi_1^0}$ plane of the allowed region represented by black circles consistent with electroweak symmetry breaking and WMAP relic density constraints of Eq.(9) for the mSUGRA case including the parameter space on the hyperbolic branch. The input parameters are the same as in Fig. 1(a)

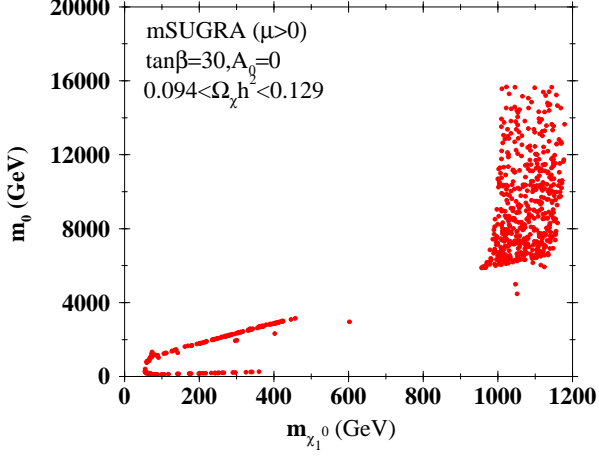


(c) Same as Fig. 1(b) except that the plot is in the $m_{\frac{1}{2}} - m_{\chi_1^0}$ plane.

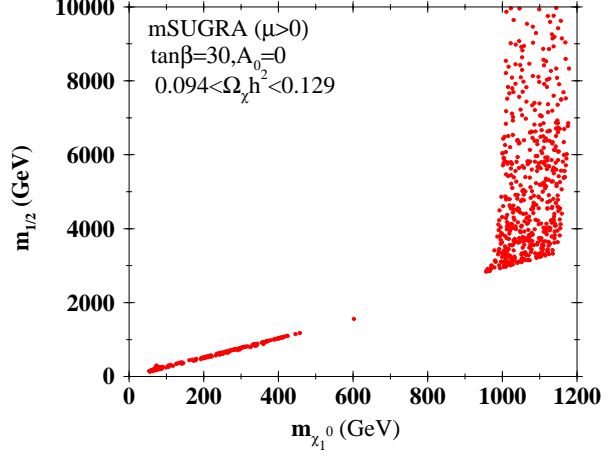
Figure 1: Relic density constraint and neutralino mass range for $\tan\beta = 10$



(a) Same as Fig. 1(a) except $\tan \beta = 30$. $b \rightarrow s + \gamma$ contour and a_μ^{SUSY} contours are also shown.

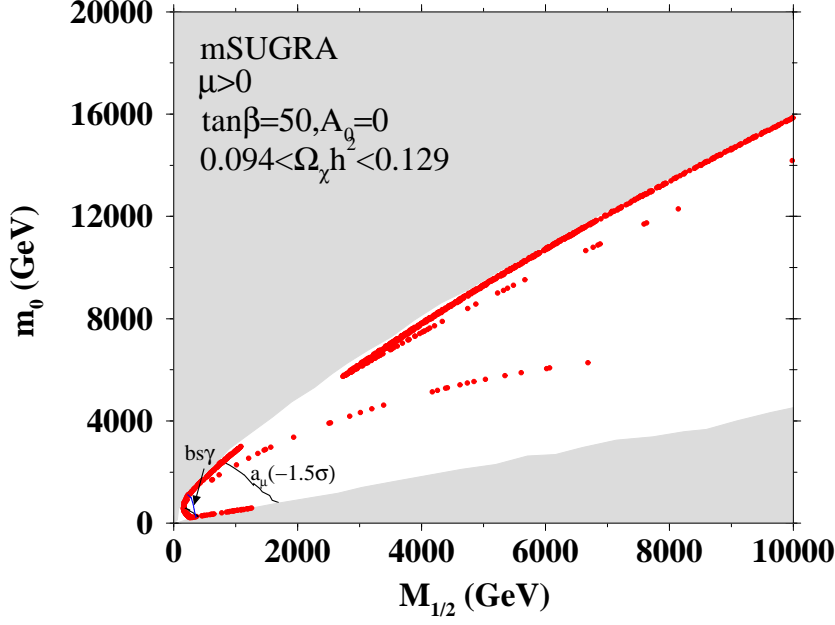


(b) Same as Fig. 1(b) except $\tan \beta = 30$.

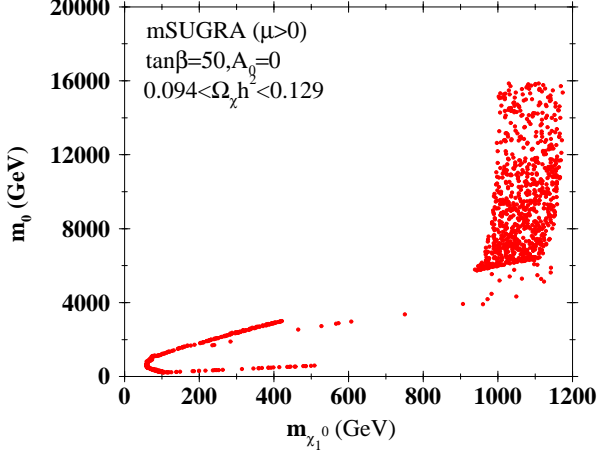


(c) Same as Fig. 1(c) except $\tan \beta = 30$.

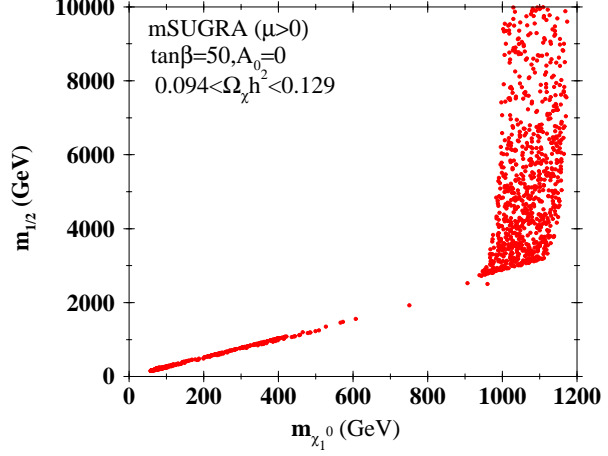
Figure 2: Relic density constraint and neutralino mass range for $\tan \beta = 30$



(a) Same as Fig. 1(a) except $\tan \beta = 50$. $b \rightarrow s + \gamma$ contour and a_μ^{SU5Y} contours are also shown.



(b) Same as Fig. 1(b) except $\tan \beta = 50$.



(c) Same as Fig. 1(c) except $\tan \beta = 50$.

Figure 3: Relic density constraint and neutralino mass range for $\tan \beta = 50$

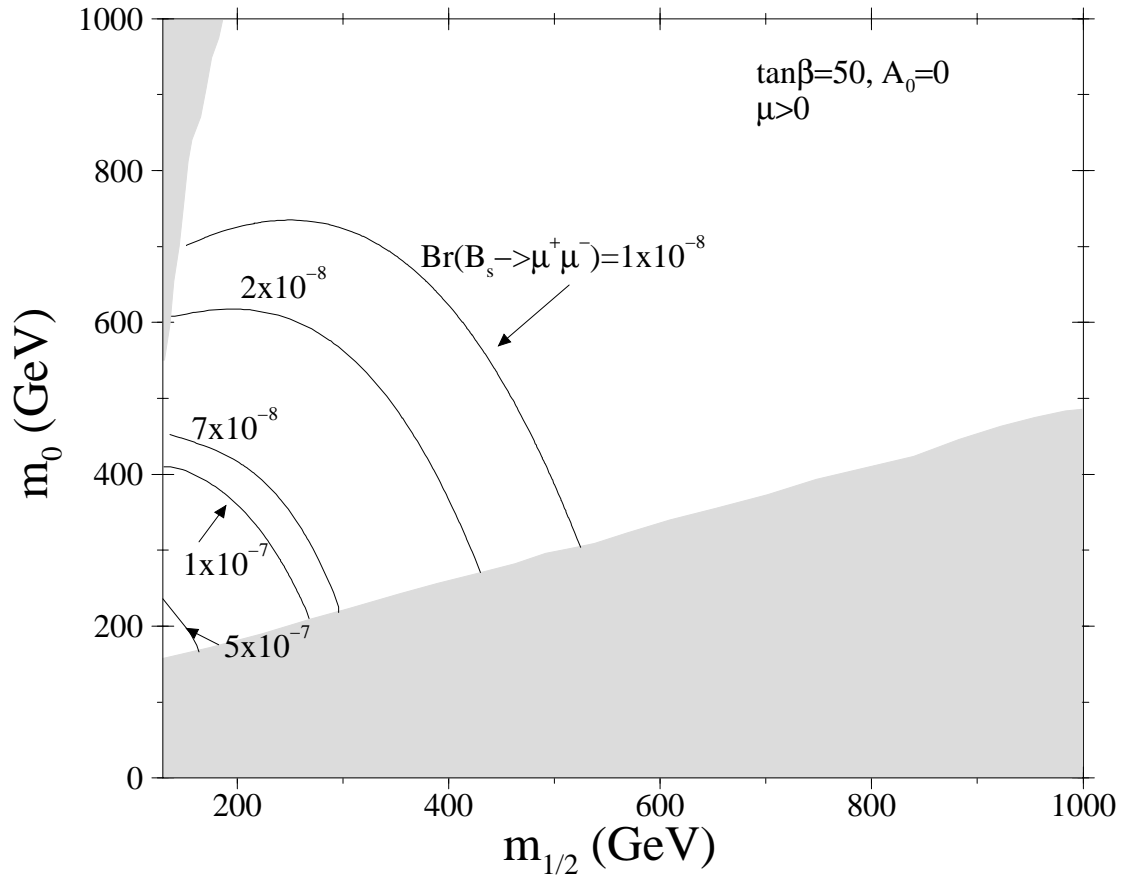
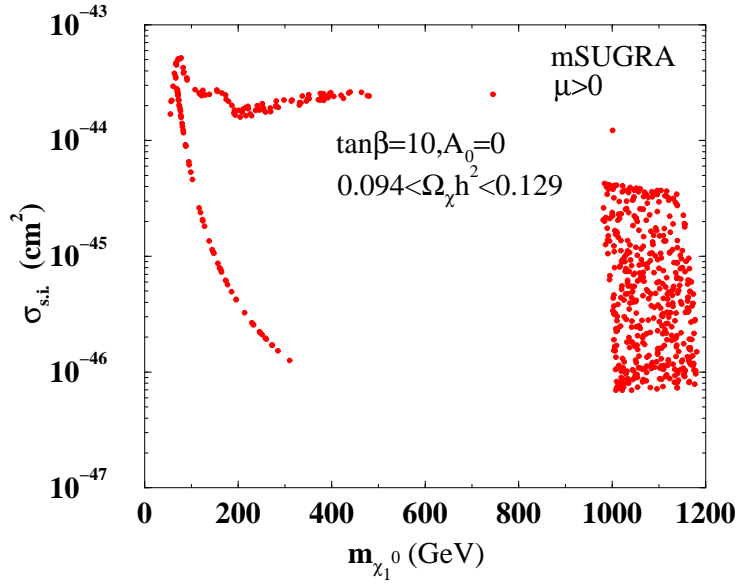
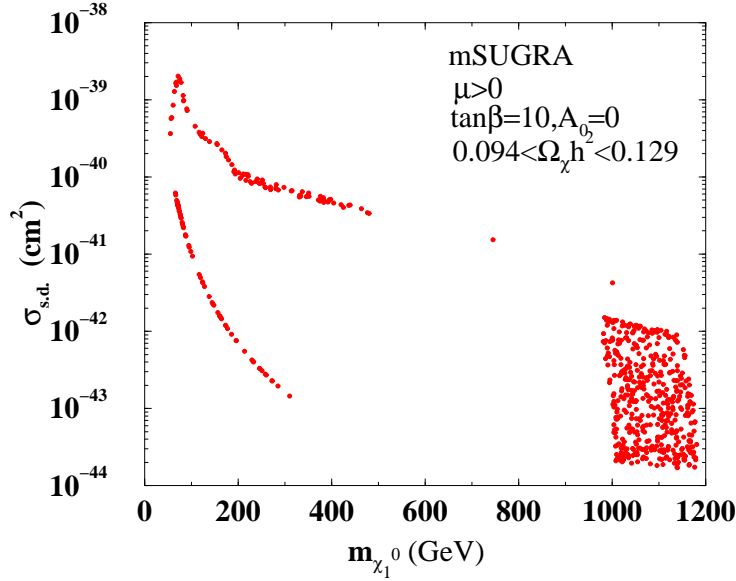


Figure 4: A plot of the $B(B_s^0 \rightarrow \mu^+ \mu^-)$ constraint in the $m_{\frac{1}{2}} - m_0$ plane.

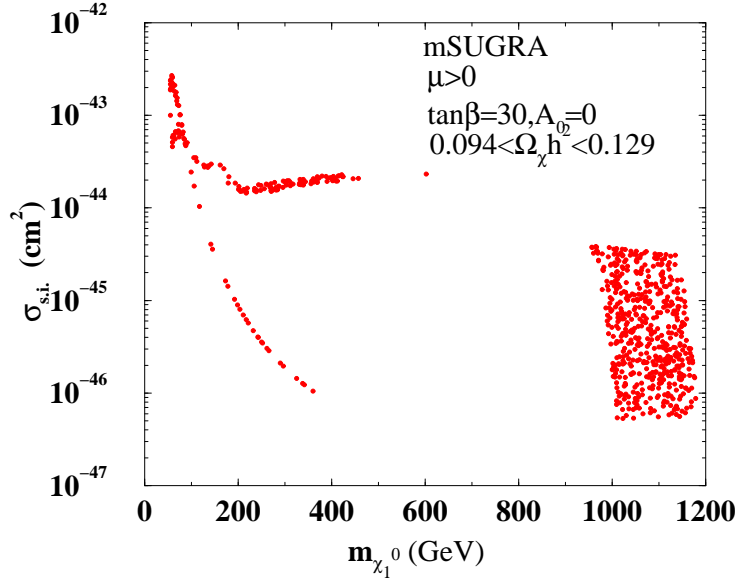


(a) A plot of the neutralino-proton spin independent cross section $\sigma_{\chi_1^0 p}(SI)$ vs the neutralino mass for the allowed region of the parameter space for all the same input parameters and constraints as in Fig. 1(a)

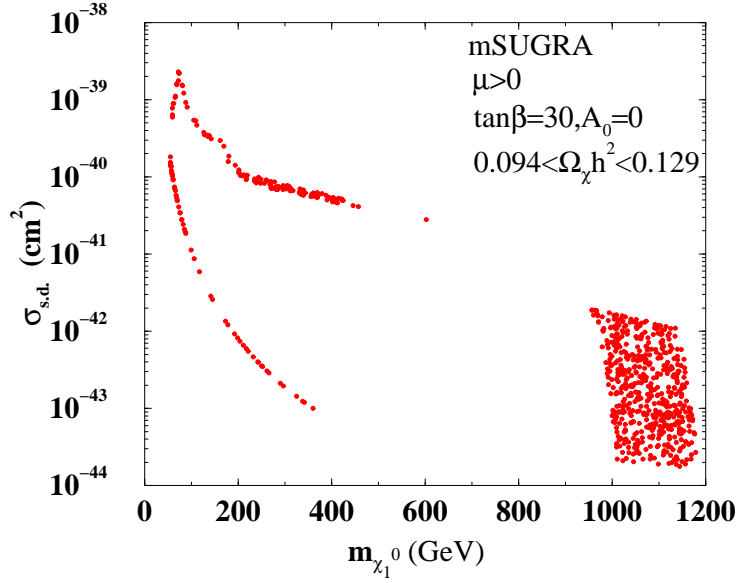


(b) A plot of the neutralino-proton spin dependent cross section $\sigma_{\chi_1^0 p}(SD)$ vs the neutralino mass for the allowed region of the parameter space for all the same parameters and constraints as in Fig. 1(a)

Figure 5: Spin Independent and Spin Dependent Cross Sections for tan $\beta = 10$

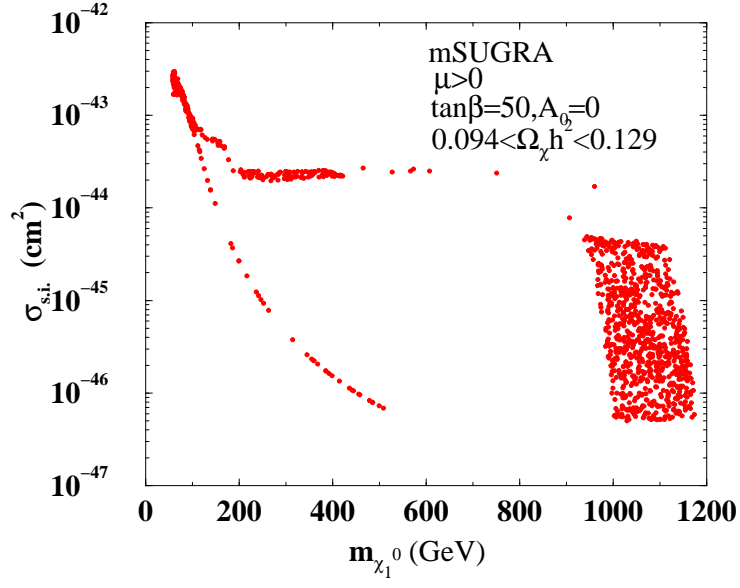


(a) Same as Fig. 5(a) except $\tan\beta = 30$.

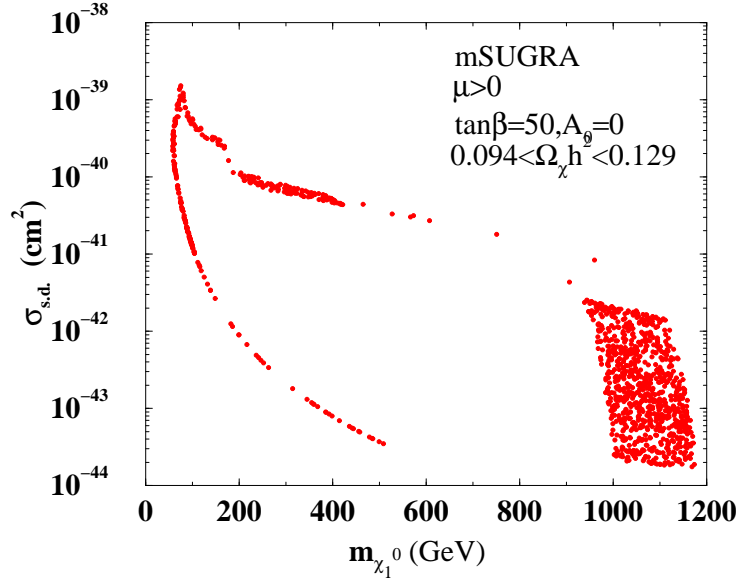


(b) Same as Fig. 5(b) except $\tan\beta = 30$.

Figure 6: Spin Independent and Spin Dependent Cross Sections for $\tan\beta = 30$



(a) Same as Fig. 5(a) except $\tan\beta = 50$.



(b) Same as Fig. 5(b) except $\tan\beta = 50$.

Figure 7: Spin Independent and Spin Dependent Cross Sections for $\tan\beta = 50$